Optica Applicata, Vol. XXXIX, No. 4, 2009

Characterization of the different energy-gap multilayer structures using near field microscopy

ANDRZEJ SIKORA[1*], ROMAN SZELOCH[2], EUGENIUSZ PROCIÓW[2]

[1]Electrotechnical Institute, Division of Electrotechnology and Materials Science,
ul. M. Skłodowskiej-Curie 55/61, 50-369 Wrocław, Poland

[2]Faculty of Microsystem Electronics and Photonics, Wrocław University of Technology,
ul. Janiszewskiego 11/17, 50-372 Wrocław, Poland

[*]Corresponding author: sikora@iel.wroc.pl

One of the materials which can be used in high-temperature electronic devices is silicon carbide (SiC). Its properties are very promising, however, a number of technological issues must be solved first, and complex phenomena connected with contact development must be investigated. In this paper, some results the measurements of electrical parameters of the silicon carbide based multilayer SiC:Zr-NiCrSi-Ag systems developed on glass substrate by magnetron co-sputtering method from compositional target are presented. This system was tested electrically as potentially useful to SiC and TiO_2 layers contact. Due to the presence of potential barriers, observed with conventional methods, one should use a more precise and sophisticated instrument. One of the important tools which can be used in order to obtain the information about morphological and electrical properties of the surface is the near-field microscopy. Two modes were used during the measurements: EFM (electrostatic force microscopy) and SP (surface potential imaging). Those techniques allow obtaining several sets of data describing different properties of the sample. Moreover, its sophisticated nature delivers the information in submicron scale and no influence on the structure and phenomena is introduced. Also the multichannel data acquisition allows a certain amount of data concerning signals to be collected, which is very useful for the analysis of results in order to identify the presence of artifacts. Some results obtained during preliminary work are hereby presented and described.

Keywords: thin films, contact phenomena, near field microscopy, AFM, silicon carbide.

1. Introduction

The development of new materials allows us to design devices which can meet the requirements of applications under harsh environmental conditions, in which the previously available devices could not be implemented. Silicon carbide (SiC) based materials show a number of properties, which opens up a new perspective for production of high-temperature transducers [1, 2], semiconductor devices [3], MEMS

and NEMS [4, 5], thermal and optical detectors, chemical sensors [6–8] and field emitters [9]. Within these applications, especially challenging in processing is to get long-term electrical stability of contact layers. The differences in emission work and electron affinity in the case of direct contact between metal and semiconductor generate voltage barriers, contact interfacial potentials and depletion layers both in the vicinity of contact and within the semiconductor body.

The interdiffusion of contact materials, so-called Kirkendall effect, and electromigration often lead to an increase of surface and volume resistances and an electrical and mechanical destruction of the contact due to the effect. The next task to cope with, when it comes to processing the contact layers, is to combine their tailored electrical properties with their thermal resistance, to ensure satisfactory operation of the materials at high temperatures. The multilayer contact with an interlayer in some way can solve the problem, as it enables the contact ohmic and Schottky barrier properties to be tailored to the needs of stability at high temperatures. It must be underlined that post processing high temperature contact forming procedure is necessary in the case of wide band materials. Presently, structures of such type, processed from SiC, can successfully work at temperatures above 500 °C.

In order to recognize the properties of those materials one needs to perform a large number of experiments, where basic parameters, interactions with other materials, reliability and other factors are measured and evaluated [10–13]. The technology of thin film preparation must be developed very carefully whether it is magnetron sputtering [14, 15] or epitaxial deposition process [16, 17]. Especially the contacts are critical structures due to various mechanisms and phenomena which must be taken into account when different materials are to be deposited in various compositions [18]. As the dimensions of the structures are smaller and smaller, and the local interactions have a strong influence on the whole device operational features, one needs high--resolution tools for measuring and imaging the properties. Therefore, the near-field techniques are very useful in both steps of development and quality control of the devices. When the electrical properties of the structure are considered [12, 15, 19], the electrostatic force microscopy (EFM) [20, 21] and surface potential imaging (SP) modes are desired [22, 23].

2. Preparation of the samples

The SiC structures were prepared by magnetron sputtering of the graphite-silicon--zircon composite target. The proportion of silicon and graphite on the target surface was such as to get stoichiometric SiC. The sputtering process was performed using a UV PLS 570 Pfeiffer device adapted to work with magnetrons. The deposition process was carried out in a vacuum chamber in an argon atmosphere of 7 to 9×10^{-4} mbar with the background pressure of residual gas 5×10^{-7} mbar. The SiC layer was deposited on Corning 7059 substrates which were subjected to a procedure of the typical wet cleaning and vacuum annealing at 600 K for 20 min prior to deposition. The magnetron cathode was supplied with a Dora power module. The device uses

600 μs unipolar voltage pulses. For the active power of 0.61 kW and plasma current 0.51 A the rate of SiC deposition was about 3.1 Å/s. The NiCrSi layers were also deposited from a composite target in an argon atmosphere of 10^{-4} mbar. For the active power of 0.59 kW and plasma current 0.51 A the rate of NiCrSi deposition was 8 to 10 Å/s. The TiO_2 layer was deposited from Ti metal target which was sputtered in a reactive atmosphere of argon and oxygen at an operating pressure of 10^{-3} mbar. For the plasma-discharge active power 0.93 kW and plasma current of 1.33 A, the rate of TiO_2 deposition was about 0.5 Å/s. The Ag layer was thermally evaporated using a molybdenum heater. During depositions the temperature of substrates was maintained in the range 570–590 K using radiation heaters. The thickness of the layers obtained was estimated using known growth ratio. It was also verified with optical interference microscopy (551 nm – filtered Hg lamp) and did not exceed the following values: TiO_2 – 500 nm, NiCrSi – 350 nm and Ag – 500 nm.

3. Measurements

The measurements of the structures were performed using the Innova system from Veeco corporation. Both modes of electrostatic force microscopy and surface potential imaging (known also as scanning Kelvin probe microscopy – SKPM) were used in order to obtain information about the properties of the surface. Pt-Ir tip-ended cantilevers with typical spring constant of about 1 N/m and the resonance frequency 60 kHz were used. Both EFM and SP measurements were performed in the tapping mode/lift mode. The measurements were carried out at ambient and room temperature. Due to the nature of the measurements, the following signals could be acquired and represented from: topography, phase shift (viscous and elastic forces), the topography error signal and the electrostatic force (when EFM measurement was performed) or topography, phase shift, the topography error signal and the surface potential (when SP measurement was performed). Electrostatic force microscopy (EFM) is a derivative technique from the intermittent contact mode, where the detection of the tips' oscillation amplitude is used for determination of the tip-to-sample distance. While scanning over the surface, one can gather information about the height at every point and create the map which images the shape of the scanned surface. The acquisition of information about the electrostatic charge is realized by moving the tip above the surface, where previously observed interaction between the tip and the sample is no longer present, but the electrostatic interaction can still be detected. Therefore, the first pass of the tip allows us to obtain information about the height of the surface, and during the second pass the tip is raised above the surface and moves along the acquired profile. A change of the amplitude and the phase shift caused by the electrostatic interaction are observed. This procedure is known as the two-pass, or the lift mode, technique. In order to perform such measurement, the silicon tip with a metallic layer deposited on it should be used and the cantilever should be connected electrically to the biasing circuit. After the measurement is complete, one obtains two maps: the topography of the sample and the charge distribution correlated with

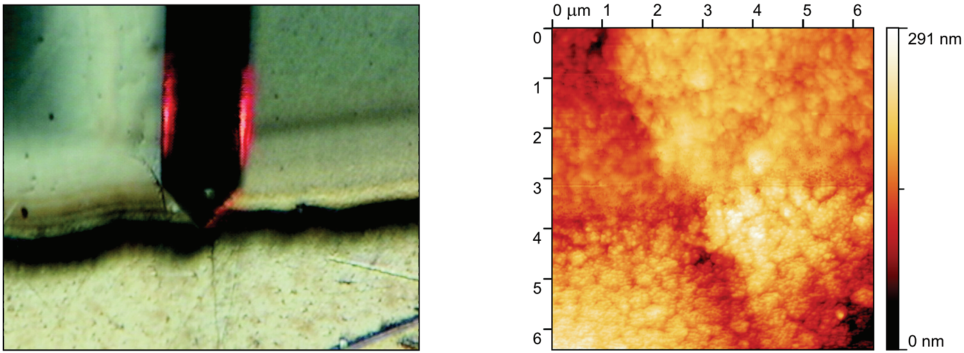

Fig. 1. Optical microscope view (left-hand side) of the cantilever placed over the surface of Ag-NiCrSi contact on an SiC:Zr layer 2 µm thick. The topography of the sample (right-hand side). Scan size: 6.5×6.5 µm.

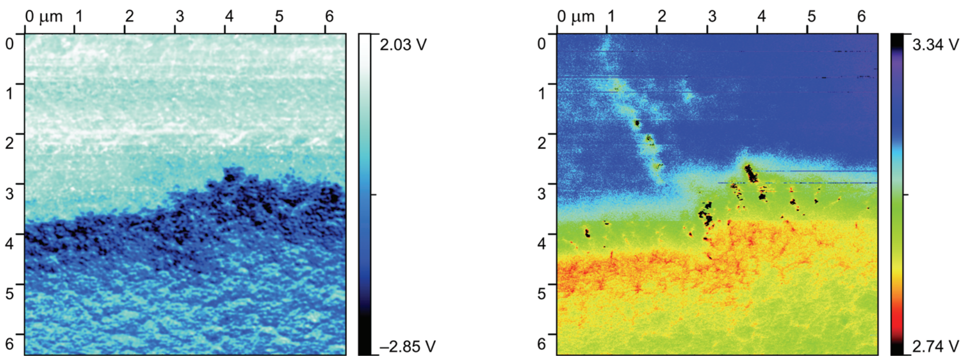

Fig. 2. Images corresponding to the topography of the surface presented in Fig. 1. Phase imaging (left-hand side) reveals the viscous and elastic forces interacting between the tip and the sample. EFM image (right-hand side). Scan size: 6.5×6.5 µm.

the topography. Figures 1 and 2 show the results of the EFM measurements of the Ag-NiCrSi contact deposited on the SiC:Zr 2 µm thick layer. In order to provide better control on tip-feature alignment, the optical view of the scanning field was used. The cantilever's position on the sample is also shown in Fig. 1.

The results show very good correlation between the topography and both phase imaging and EFM signals. One can easily see the horizontal line between the two layers. In the topography, one can distinguish two different areas due to the difference in roughness. The upper area is more flat; however it reveals also the structures of the lower part which is the substrate. A vertical line is only a feature related to the substrate shape. It has no influence on the other properties of the sample. A phase imaging picture in Fig. 2 shows differences in material due to its different viscous and elastic interaction with the scanning tip, and clearly reveals the border between the areas. Also some transient area (the darkest line) can be distinguished. The most interesting image was obtained using EFM mode. One can see different potentials

present in those areas. It must be emphasized that the sample was not biased, therefore the measurement result appeared due to phenomena connected with charge generation in the contact area. The primary conclusion is that observed phenomena were caused by charge separation (hot electrons separation). This measurement confirmed the measurements performed with standard equipment.

Although the EFM delivers interesting insight into the submicron distribution of the electrical properties, one cannot consider it as quantitative information without performing a complex and time consuming measurement. In order to overcome this issue, SP imaging can be used. This method maps the electrostatic potential of the sample surface (and can reveal contact potential differences). As the tip is travelling above the surface in lift mode, the tip and cantilever experience a force wherever the potential at the surface is different than the potential of the tip. The force is nullified by varying the voltage of the tip so that the tip be at the same potential as the region of the sample surface underneath it. Figures 3 and 4 present results of the measurements of contact structures NiCrSi:TiO_2. One can see in the topography the height difference

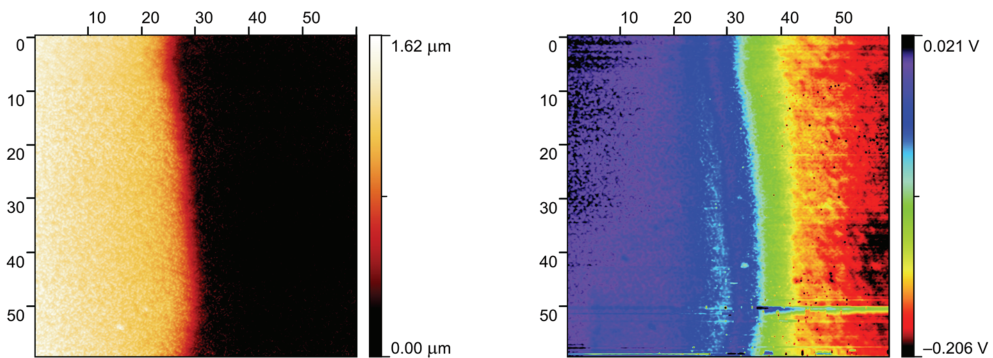

Fig. 3. Topography of the NiCrSi:TiO_2-sample surface (left-hand side). Surface potential imaging (right- hand side). Scan size: 60×60 μm.

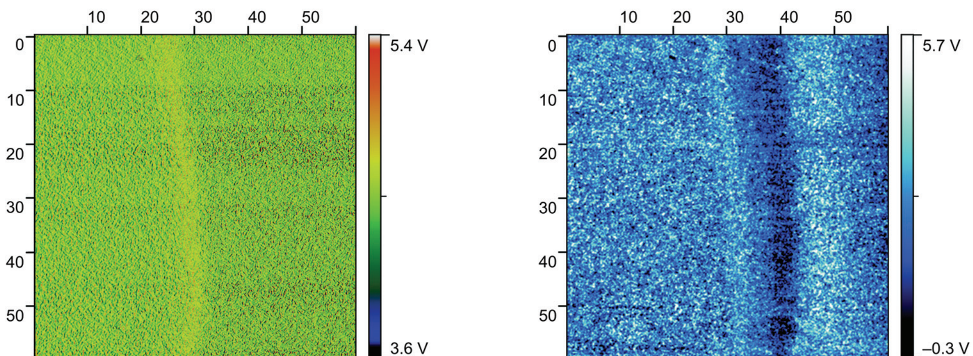

Fig. 4. The error of topography scan of the NiCrSi:TiO_2-sample surface (left-hand side). Phase imaging (right-hand side). Scan size: 60×60 μm.

between the two layers as well as a difference in the grain structure. Therefore, we could confirm the presence of an interesting feature within the scanning field. The SP image reveals the presence of electrical field, with the voltage difference about 220 mV, which correlates with macroscopic measurements.

Figure 4 shows additional signals which are helpful in checking if any artifact appeared in the previous pictures. The error signal which shows if the sample was scanned properly and if the topography as well as the surface potential signal were distorted due wrong PID settings (proportional-integral-derivative regulator responsible for keeping the tip-sample distance at constant value), does not show any significant features. The only visible line is along the edge of the top contact layer. This indicates that the SP map, showing a dual change of the potential, could be convoluted by imperfection of maintaining tip-sample distance. One can also see a relatively large amplitude of error signal. The reason of such a result was a relatively large roughness of the surface and fast scanning. Much more interesting is the phase imaging map, which usually shows the same features as error signal, but generally it reveals the differences in adhesion and elasticity of the surface. In the result presented, there was no correlation to the error signal, but the vertical line shows some specific area on the right to the contact. It could be caused by a locally increased viscosity (due to the presence of some contamination possibly connected with the mask used for deposition of the upper layer of contact). This line correlates with the surface potential map showing also a line in this area, which means that the fluctuation revealed had also an impact on the distribution of electric properties. One can see that access to the different signals acquired during the measurement can help in the analysis of result. Also, the force-distance spectroscopy would be useful in this case in order to identify the nature of the feature revealed by phase imaging. The grainy structure is clearly visible in Fig. 5, where both lower and upper one of the contact were magnified. The shape of grains of the lower (TiO_2) layer is very specific and, according to some papers, it causes the separation of hot electrons and appearance of such voltage value in the contact area.

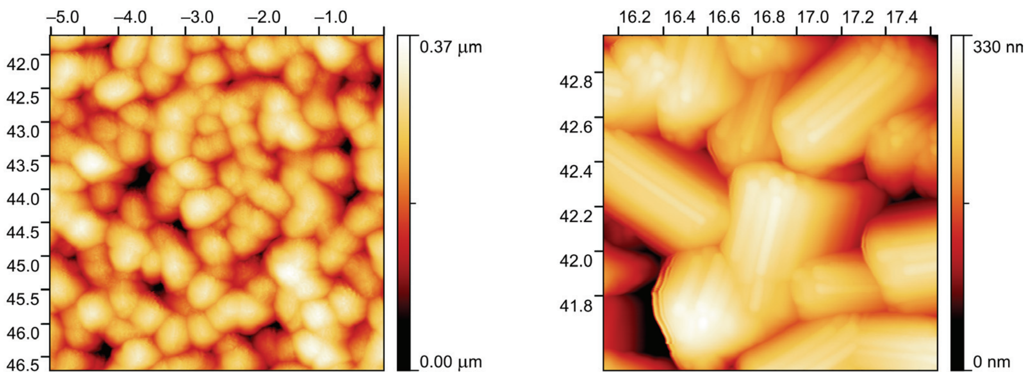

Fig. 5. Ag-NiCrSi contact deposited on TiO_2 layer: topography of the Ag-NiCrSi layer (left-hand side), TiO_2 layer (right-hand side). Scan size: 5×5 µm and 1.5×1.5 µm, respectively.

4. Summary and outlook

The structures developed show very interesting properties, which requires further investigation with various techniques. It should be underlined that such promising results allow predicting implementation of devices based on those or similar multilayer contacts. By performing the measurements with a typical equipment (power units, meters) we could obtain primary data which brought our attention to the developed structures. As the next step, the near-field microscopy techniques were used in order to provide more detailed information.

Examples of the results obtained show the advantages of using the near-field microscopy techniques in material and structure tests. The most important advantage of the method is the non-contact measurement of the presence of the electric potential in the structure. Although one can use the large internal-resistance voltmeter (*i.e.*, electrometer) to observe the phenomena in question, some influence of the measuring device on the observed object must be taken into account. Unlike the classic methods, the near field techniques can reveal such sophisticated phenomena without disturbing the condition on the surface. Moreover, when the typical method is applied, one must develop contacts to particular areas. Using typical, hand operated probes can cause contamination of the object as well as mechanical and chemical modification of the contact areas on the surface. Such issues in some cases are not accepted. Moreover, the AFM techniques make it possible to visualize the distribution of certain properties along the surface and to correlate them to each other (topography with paying attention to the structures of grains, the phase imaging correlated with the viscous and elastic forces and the electrostatic forces) with submicron resolution. Also, analysis of other signals is important in order to investigate the possible presence of artifacts. Further work is to be carried out in order to test various solutions.

Acknowledgements – This work was supported by the Polish Ministry of Scientific Research and Information Technology within a statute research of the Electrotechnical Institute, Wrocław, Project No. 500-8520-26.

References

[1] MOLLER S., LIN J., OBERMEIER E., *Material and design considerations for low-power microheater modules for gas-sensor applications*, Sensors and Actuators B: Chemical **25**(1–3), 1995, pp. 343–346.

[2] WICHE G., BERNS A., STEFFES H., OBERMEIER E., *Thermal analysis of silicon carbide based micro hotplates for metal oxide gas sensors*, Sensors and Actuators A: Physical **123–124**, 2005, pp. 12–17.

[3] MURARKA S.P., *Silicide thin films and their applications in microelectronics*, Intermetallics **3**(3), 1995, pp. 173–186.

[4] CIMALLA V., PEZOLDT J., AMBACHER O., *Group III nitride and SiC based MEMS and NEMS: materials properties, technology and applications*, Journal of Physics D: Applied Physics **40**(20), 2007, pp. 6386–6434.

[5] ILIESCU C., CHEN B., *Thick and low-stress PECVD amorphous silicon for for MEMS applications*, Journal of Micromechanics and Microengineering **18**(1), 2008, p. 015024.

[6] WRIGHT N.G., HORSFALL A.B., *SiC sensors: a review*, Journal of Physics D: Applied Physics **40**(20), 2007, pp. 6345–6354.

[7] FAWCETT T.J., WOLAN J.T., MYERS R.L., WALKER J., SADDOW S.E., *Wide-range (0.33%–100%) 3C–SiC resistive hydrogen gas sensor development*, Applied Physics Letters **85**(3), 2004, pp. 416–419.

[8] SPETZ A.L., UNEUS L., SVENNINGSTORP H., TOBIAS P., EKEDAHL L.-G., LARSSON O., GORAS A., SAVAGE S., HARRIS C., MARTENSSON P., WIGREN R., SALOMONSSON P., HAGGENDAHL B., LJUNG P., MATTSSON M., LUNDSTROM I., *SiC based field effect gas sensors for industrial applications*, Physica Status Solidi (a) **185**(1), 2001, pp. 15–25.

[9] GÓRECKA-DRZAZGA A., DZIUBAN J., BARGIEL S., PROCIÓW E., *Mold-type SiC emitters with nanoholes at the apex*, Measurements Science and Technology **17**(1), 2006, pp. 45–49.

[10] JANZEN E., HENRY A., BERGMAN J.P., ELLISON A., MAGNUSSON B., *Material characterization need for SiC-based devices*, Materials Science in Semiconductor Processing **4**(1–3), 2001, pp. 181–186.

[11] MOHNEY S.E., HULL B.A., LIN J.Y., CROFTON J., *Morphological study of the Al–Ti ohmic contact to p-type SiC*, Solid-State Electronics **46**(5), 2002, pp. 689–693.

[12] BISWAS N., WANG X., GANGOPADHYAY S., *Electrical properties of amorphous silicon carbide films*, Applied Physics Letters **80**(18), 2002, pp. 3439–3442.

[13] BERLIND T., HELLGREN N., JOHANSSON M.P., HULTMAN L., *Microstructure, mechanical properties, and wetting behavior of Si–C–N thin films grown by reactive magnetron sputtering*, Surface and Coatings Technology **141**(2–3), 2001, pp. 145–155.

[14] KIKUCHI N., KUSANO E., TANAKA T., KINBARA A., NANTO H., *Preparation of amorphous* $Si_{1-x}C_x$ *(*$0 \leq x \leq 1$*) films by alternate deposition of Si and C thin layers using a dual magnetron sputtering source*, Surface and Coatings Technology **149**(1), 2002, pp. 76–81.

[15] WANG M., HUANG A.P.,WANG B., YAN H., YAO Z.Y., MORIMOTO A., SHIMIZU T., *Bias effects on structure of sputtered SiC films*, Materials Science and Engineering B **85**(1), 2001, pp. 25–27.

[16] FISSELA A., KAISERA U., SCHROTERA B., RICHTERA W., BECHSTEDT F., *MBE growth and properties of SiC multi-quantum well structures*, Applied Surface Science **184**(1–4), 2001, pp. 37–42.

[17] NEYRET E., DI CIOCCIO L., BLUET J.M., PERNOT J., VICENTE P., ANGLOS D., LAGADAS M., BILLON T., *Deposition, evaluation and control of 4H and 6H SiC epitaxial layers device application*, Materials Science and Engineering B **80**(1–3), 2001, pp. 332–336.

[18] CROFTON J., MOHNEY S.E., WILLIAMS J.R., ISAACS-SMITH T., *Finding the optimum Al–Ti alloy composition for use as an ohmic contact to p-type SiC*, Solid-State Electronics **46**(1), 2002, pp. 109–113.

[19] TARNTAIR F.G., WU J.J., CHEN K.H., WEN C.Y., CHEN L.C., CHENG H.C., *Field emission properties of two-layer structured SiCN films*, Surface and Coatings Technology **137**(2–3), 2001, pp. 152–157.

[20] STERN J.E., TERRIS B.D., MAMIN H.J., RUGAR D., *Deposition and imaging of localized charge on insulator surfaces using a force microscope*, Applied Physics Letters **53**(26), 1988, pp. 2717–2719.

[21] TERRIS B.D., STERN J.E., RUGAR D., MAMIN H.J., *Localized charge force microscopy*, Journal of Vacuum Science and Technology A **8**(1), 1990, pp. 374–377.

[22] NONNENMACHER M., O'BOYLE M.P., WICKRAMASIGHE H.K., *Kelvin probe force microscopy*, Applied Physics Letters **58**(25), 1991, pp. 2921–2923.

[23] JACOBS H.O., KNAPP H.F., MULLER S., STEMMER A., *Surface potential mapping: A qualitative material contrast in SPM*, Ultramicroscopy **69**(1), 1997, pp. 39–49.

Received June 19, 2009
in revised form October 6, 2009